Ind. Basis - 4112

NATIONAL ADVISORY COMMITTEE FOR AERONAUTICS

TECHNICAL NOTE

No. 1676

GRAPHICAL METHOD OF OBTAINING THEORETICAL LIFT DISTRIBUTIONS ON THIN WINGS AT SUPERSONIC SPEEDS

By Clarence B. Cohen and John C. Evvard

Flight Propulsion Research Laboratory
Cleveland, Ohio

Washington
August 1948

NATIONAL ADVISORY COMMITTEE FOR AERONAUTICS

TECHNICAL NOTE NO. 1676

GRAPHICAL METHOD OF OBTAINING THEORETICAL LIFT DISTRIBUTIONS ON THIN WINGS AT SUPERSONIC SPEEDS

By Clarence B. Cohen and John C. Evvard

SUMMARY

A graphical method is presented for calculating the linearized lift distribution on thin wings at supersonic speeds. The technique may be applied to all wing regions except those influenced by interacting flow fields off the wing-plan boundaries. The lifting-pressure coefficients are obtained as the sum of a graphical line integration and several terms that are functions of only the plan form.

Pressure coefficients obtained by the graphical method for a swept trapezoidal wing and for a wing with straight-swept leading edge and parabolic wing-tip are compared with those derived by closed-form integration. The lift distributions for two plan forms previously unsolved are also included.

INTRODUCTION

The evaluation of the theoretical performance of arbitrarily shaped wings at supersonic speeds has been retarded by the complexities involved in analysis when the wing boundaries are other than certain prescribed curves, usually straight lines. Solutions for the velocity potential on an arbitrary wing surface are presented in references 1 and 2 except for those regions influenced by interacting flow fields off the wing-plan boundaries; the integrals involved, however, have been tabulated only for special plan forms. Although the integrals may be so reduced that numerical evaluation of the velocity potential is feasible, the procedure for obtaining the lift distribution requires an additional numerical partial differentiation that is cumbersome and of doubtful accuracy.

The lift distributions for a family of thin wings may be obtained by the methods of reference 2 as the sum of an algebraic function and a line integral. The line integral may be evaluated by numerical or graphical methods.

A graphical method formulated at the NACA Cleveland laboratory for evaluating the lift distribution for wings of arbitrary plan form within the limitations of reference 2 is presented. Also included for a Mach number of $\sqrt{2}$ are curves showing the relations between the algebraic functions and the geometry of the wing. The application of the method to the various types of region encountered in analyses of general wings is discussed. As illustrations, the pressure coefficients obtained by this graphical method are compared with those derived by closed-form integration for a swept trapezoidal wing and for a wing with a straight leading edge and parabolic wing-tip boundaries. Lift distributions of two other plan forms are also included to illustrate the application of the method.

SYMBOLS

The following symbols and subscripts are used in this report:

$a_2, a_3, \ldots, a_n$	coefficients in series expansion defining curvature of leading edge
a', b', c', d'	quantities used in determining factor ΔF_2
$C_1 \ldots C_n$	coefficients in series representation of ΔF_2
C_p	pressure coefficient
ΔC_p	contribution to C_p of portion of leading edge included in segment of width ϵ
F_1	factor representing integral-function contribution to C_p
F_2	factor representing contribution of integration over width ϵ to C_p
ΔF_2	error in F_2 due to neglecting curvature
H	quantity representing numerical integration along leading edge, $\Delta\eta\Sigma h$
h	parameter defining equilateral hyperbola
k_1	constant determining sweep of straight leading edge

M	free-stream Mach number
m	slope of wing edge, $\frac{dy}{dx}$
$Q(\epsilon)$	series defining curvature of leading edge
R	ratio of distances, $\frac{v_w - v_1(u_2)}{u_w - u_2}$
r	local radius of curvature
U	free-stream velocity (parallel to x-axis)
u, v	oblique coordinates whose axes lie parallel to Mach lines
$u_2(v)$ or $v_2(u)$	equation of tip and trailing edge of wing
$v_1(u)$ or $u_1(v)$	equation of supersonic leading edge of wing (inboard of foremost tangent Mach wave)
x, y	Cartesian coordinates
y'	transformed y-coordinate
α	angle of attack, radians
β =	$\sqrt{M^2 - 1}$
ϵ	width of strip chosen in evaluating F_2
θ_1, θ_2	local angles between wing edge and free-stream flow direction
ξ, η	Cartesian coordinates of point sources
φ	perturbation-velocity potential

Subscripts:

0	intersection of grid edge with wing-plan boundary
L	leading edge of wing

l	left
r	right
w	wing

ANALYSIS

As a result of the linearized theory, the effect of angle of attack on the lift distribution of thin wings at supersonic speeds depends upon the plan-form boundaries and is independent of the wing-section slopes. Determination of the pressure distribution of a thin flat plate therefore solves the problem of the lift distribution of the finite-thickness wing. Reference 2 shows that the local pressure coefficients of several classes of wings with arbitrary plan boundaries may be evaluated by line integrals of explicit functions.

A graphical method of evaluating the lift-distribution functions presented in reference 2 is developed herein. In order to illustrate the method developed, a simple wing including regions influenced by a supersonic leading edge, a subsonic leading edge, and a subsonic trailing edge (fig. 1) is discussed in detail. The essential elements in the calculations for each region are included in the analysis for the region B influenced by the subsonic leading edge.

The pressure coefficient for region B as derived in reference 2 is

$$C_p = -\frac{M\alpha}{\pi\beta}\left[\int_{ab} \frac{d\eta}{\sqrt{(u_w - u)\,(v_w - v)}} + \frac{2}{M}\left(1 - \frac{du_2}{dv_w}\right)\sqrt{\frac{v_w - v_1(u_2)}{u_w - u_2}}\right] \tag{1}$$

where u_2 is evaluated at $v = v_w$. Except for the symbol η, equation (1) is expressed in a set of oblique coordinates (fig. 2) whose axes are parallel to the Mach lines. The transformation equations relating the oblique and Cartesian coordinates are

$$\left.\begin{aligned} u &= \frac{M}{2\beta}(\xi - \beta\eta) & v &= \frac{M}{2\beta}(\xi + \beta\eta) \\ \xi &= \frac{\beta}{M}(v + u) & \eta &= \frac{1}{M}(v - u) \\ u_w &= \frac{M}{2\beta}(x - \beta y) & v_w &= \frac{M}{2\beta}(x + \beta y) \\ x &= \frac{\beta}{M}(v_w + u_w) & y &= \frac{1}{M}(v_w - u_w) \end{aligned}\right\} \quad (2)$$

The significance of the terms of equation (1) is clarified in figure 3. The line integral is to be evaluated along the portion of the supersonic leading edge from a to b. The quantity $[v_w - v_1(u_2)]$ can be interpreted as distance $\overline{bc}$ and the quantity $(u_w - u_2)$ can be interpreted as the distance $\overline{cP}$. The ratio of these distances is called R. For a given Mach number, the quantity $\left(1 - \frac{du_2}{dv_w}\right)$ depends upon only the slope of the wing boundary at the point (u_2, v_w).

By use of equations (2), the second term of equation (1) may be expressed in terms of R and the angle θ_1 that the wing edge makes with the free-stream flow direction (parallel to the x-axis) as

$$F_1 = \frac{2}{M}\left(1 - \frac{du_2}{dv_w}\right)\sqrt{R}$$

$$= \frac{4\beta}{M}\frac{\tan\theta_1}{(\beta\tan\theta_1 + 1)}\sqrt{R} \quad (3)$$

where θ_1 is positive counterclockwise. This expression, evaluated for $M = \sqrt{2}$, appears in figure 4.

The quantities $(u_w - u)$ and $(v_w - v)$ in the line integral of equation (1) are the coordinate distances (fig. 3) of each element $d\eta$ to the point (u_w, v_w). The curves of

$$\frac{1}{\sqrt{(u_w - u)(v_w - v)}} = \text{constant} = h$$

in the u,v coordinate system are a family of equilateral hyperbolas asymptotic to the lines $u = u_w$, $v = v_w$. A family of these hyperbolas is shown in figure 5.

If a "grid" of this type is placed with its origin at (u_w, v_w) and so alined that its axes are parallel to the u and v axes, the value of $\frac{1}{\sqrt{(u_w - u)(v_w - v)}}$ for any element $d\eta$ (or dy) is the constant h for the hyperbola passing through that element. The sum of the values of h taken near the center of each element for equal increments $d\eta$ along the wing boundary then evaluates the line integral of equation (1). The superposition of a wing-plan boundary on a hyperbolic grid for $M = \sqrt{2}$ is shown in figure 6. A constant value of $\Delta\eta$ is marked on the grid for convenience in summation. A part of the grid employed for calculations at $M = \sqrt{2}$ appears in figure 7.

As shown in figure 5, the value of h increases to infinity as the edge of the grid is approached. In order to perform a numerical integration, the infinities must be excluded. Therefore the numerical summation should not start with element 1 (fig. 6) but should skip a distance large enough to enable the element value to be easily determined. The part of the integral omitted must be compensated by an analytical expression that represents the contribution of a section of the leading edge $\overline{aa'}$ included in a strip of width ϵ (fig. 6).

The contribution to the line integral of the strip of width ϵ may be evaluated by assuming the wing boundary to be a straight line near $u = u_w$. From the derivation presented in appendix A, this contribution is

$$F_2 = \frac{4\beta m}{M\sqrt{(m\beta - 1)(m\beta + 1)}} \tan^{-1}\left[\frac{2\beta m(v_w - v_0)}{M\epsilon(1 + \beta m)} - 1\right]^{-\frac{1}{2}} \qquad (4)$$

where $m = \frac{dy}{dx}$, the tangent of the angle θ_2 (positive counterclockwise) that the leading edge makes with the flow direction at the intersection with the edge of the grid (point a, fig. 6), and $(v_w - v_0)$ is the distance $\overline{aP}$ from that point to the grid origin (fig. 6). The value of F_2 for various values of θ_2, $(v_w - v_0)$,

and ϵ is shown in figure 8 for $M = \sqrt{2}$. The dashed line in figures 8(b) and 8(c) represents the limit for which the arc-tangent term in equation (4) is real.

For the subsonic leading edge (region B, fig. 1), equations (1), (3), and (4) may be combined and the expression for the pressure coefficient becomes

$$C_p = - \frac{M\alpha}{\pi\beta} (H + F_1 + F_2) \tag{5}$$

where the numerical summation along the leading edge is represented by

$$H = \Delta\eta \ (h_1 + h_2 + h_3 + \ . \ . \ .) = \Delta\eta\Sigma h$$

If nonuniform increments of η are desired, a weighting of each value of h is required.

The analysis of the region of a wing tip influenced by a subsonic trailing edge (region C, fig. 1) may be appreciably shortened if the Kutta-Joukowski condition is imposed. In reference 2, it is shown that the solution which satisfies the Kutta-Joukowski condition does not contain the term F_1. Therefore F_1 is taken as zero in this region and the remaining evaluation is unchanged.

When evaluating C_p in a region where $v<0$ (region A, fig. 1, or fig. 9), the value F_1 does not exist because no subsonic leading edge is included in the forward Mach cone from point P. The integration must be conducted over the entire wing leading edge between the limits of the grid a and b. Because h becomes infinite at the right as well as at the left limit of the grid, a part of the integration at the right must be replaced by an analytical expression similar to equation (4). Equation (4) can be shown to hold at this limit if $(u_w - u_0)$ is substituted for $(v_w - v_0)$ and $(180^\circ - \theta_1)$ is substituted for θ_2. If the value of this expression is designated $F_{2,r}$ the pressure coefficient in the region where $v<0$ becomes

$$C_p = - \frac{M\alpha}{\pi\beta} (H + F_2 + F_{2,r}) \tag{5a}$$

In general, a complete wing in supersonic flow may have regions under the influence of both wing tips. A summary of the method of

obtaining lift distributions in the various types of flow field commonly encountered is given in appendix B. Also included is a numerical evaluation of the pressure coefficient at point P of figure 10.

The effect of Mach number on lift distribution for a given plan form may be determined by two alternate procedures. One method is to construct an integration grid and curves of F_1 and F_2 for the Mach number desired. If a large number of analyses at a given Mach number are to be made, this method may be preferable. If only a very few analyses at a given Mach number are to be made, however, the grid and curves of F_1 and F_2 may be used as constructed for $M = \sqrt{2}$, provided that compensating corrections are made. These corrections consist in: (1) so transforming the wing boundary that $y' = \beta y$; and (2) analyzing the wing as at $M = \sqrt{2}$ and dividing the resultant C_p/α by the value of β.

Some considerations that simplify the application of the method appear in appendix C. Construction of the integration grid, choice of $\Delta\eta$ and ϵ, drawing size, and a special example of the subsonic trailing edge are discussed.

ACCURACY OF METHOD

In order to determine the accuracy of the method, the pressure coefficient at points on two wings for which analytical expressions were obtainable were graphically computed and compared with the analytical values. The wings and the points considered appear in figure 11. The leading edges of both wings are swept back 30° and are the same except that wing A has a straight tip and wing B has a parabolic tip passing through similar points on the leading and trailing edges. The points considered are at the same x,y values for each wing. The results of the computations for C_p are presented in table I.

The magnitude of the personal error incurred in application of the method was evaluated by trial. Values of C_p/α were independently obtained by nonprofessional personnel using the graphical method, and were also analytically calculated. For wing A, the results of one of the computers contained an average error of 0.46 percent and a maximum error of 0.71 percent (table I). Another computer averaged an error of 0.53 percent with a maximum error of 1.52 percent. Results of wing B gave about the same accuracy (table I). These results were obtained from drawings with a wing chord of

$4\frac{1}{2}$ inches. The computers estimated a time rate of approximately 5 minutes per point when a large number of points were being analyzed.

Inasmuch as the first-order expression for F_2 (which also includes higher-order terms) assumed a straight leading edge, this expression was exact for the wings shown in figure 11. The accuracy of this expression for a curved edge has been investigated and is shown in appendix A. For a parabolic leading edge, the error ΔF_2 in F_2 (including fourth-order terms) as a function of the ratio ϵ/r_0 (where r_0 is the radius of curvature) is presented in figure 12. If ϵ/r_0 is small, the error in F_2 due to curvature will be small except when θ_2 approaches the Mach angle, as indicated in figure 12. The corresponding error in C_p will, of course, be a smaller percentage. A similar trend probably holds for edges of different curvature.

APPLICATIONS

As examples of the method, the lift distributions $2C_p/\alpha$ of a circular-plan-form wing and a straight wing with a circular tip are shown in figures 13 and 14, respectively, at $M = \sqrt{2}$.

For the circular wing, in the region inboard of station D, the pressure at a given chordwise station increases in the outboard direction. For a given spanwise station, the pressure is a maximum at the leading edge and drops off in the flow direction. The rate of this decrease is a minimum at the wing root.

Lines of constant pressure for the circular-tip wing swept back 30° at a Mach number of $\sqrt{2}$ are shown in figure 14. The Kutta-Joukowski condition was assumed for analysis of regions influenced by the subsonic trailing edge. The only region of high pressures and high pressure gradients is a small leading-edge region between the tangency of the foremost Mach wave and the start of the subsonic trailing edge. The pressure gradient over most of the tip is roughly in the spanwise direction.

CONCLUDING DISCUSSION

A graphical method based on linearized supersonic-flow theory has been developed for calculating the lift distributions on thin

wings at supersonic speeds. The method is applicable to all of the regions of arbitrary wings except those affected by interacting flow fields off the wing-plan boundaries. The determination of the lifting-pressure coefficient for a given point has been found to require 5 to 10 minutes with a resultant average error of less than 1 percent as determined by comparison with known analytical solutions.

Flight Propulsion Research Laboratory,
National Advisory Committee for Aeronautics,
Cleveland, Ohio, May 13, 1948.

APPENDIX A

CONTRIBUTION TO C_p OF LEADING-EDGE SEGMENT INCLUDED IN STRIP OF WIDTH ϵ

In order to determine the contribution to C_p of a segment of width ϵ, the integral of equation (1) must be evaluated. In the x,y coordinate system, this integral is

$$\Delta C_p = -\frac{2\alpha}{\pi} \int \frac{d\eta}{\sqrt{(x - \xi)^2 - \beta^2 (y - \eta)^2}} \tag{A1}$$

The integral is considered in the region near

$$(x - \xi_0)^2 - \beta^2 (y - \eta_0)^2 = 0 \tag{A2}$$

The subscript 0 refers to the point of intersection of the grid edge and the wing-plan boundary. In particular, the positive root that defines the left forward Mach line from the point (x,y) is

$$(x - \xi_0) = \beta (y - \eta_0) = \frac{\beta}{M} (v_w - v_0) \tag{A3}$$

Treatment of ϵ as a variable in the vicinity of the point (η_0, ξ_0) yields

$$\left.\begin{aligned} \eta &= \eta_0 + \epsilon \\ \xi &= \xi_0 + \frac{\epsilon}{m} + Q(\epsilon) \end{aligned}\right\} \tag{A4}$$

where

$$m = \left(\frac{d\eta}{d\xi}\right)_0$$

and

$$Q(\epsilon) = a_2\epsilon^2 + a_3\epsilon^3 + a_4\epsilon^4 + \ldots$$

Substitution of equation (A4) in equation (A1) gives

$$\frac{-\pi(\Delta C_p)}{2\alpha} = \int_0^{\epsilon} \frac{d\epsilon}{\sqrt{\left[x - \xi_0 - \frac{\epsilon}{m} - Q(\epsilon)\right]^2 - \beta^2 (y - \eta_0 - \epsilon)^2}} \tag{A5}$$

Now, if $Q(\epsilon) = 0$, the leading edge is straight and the integral may be written

$$-\frac{\pi}{2\alpha}(\Delta C_p) = \int_0^{\epsilon} \frac{d\epsilon}{\sqrt{\epsilon\left\{\left(\frac{1 - m^2\beta^2}{m^2}\right)\epsilon + \left[2\beta^2 (y - \eta_0) - \frac{2(x - \xi_0)}{m}\right]\right\}}} \tag{A6}$$

which becomes

$$\Delta C_p = -\frac{2\alpha}{\pi}\left\{\frac{2m}{\sqrt{(m\beta - 1)(m\beta + 1)}} \tan^{-1}\left[\frac{2\beta m (v_w - v_0)}{M\epsilon (1 + \beta m)} - 1\right]^{-\frac{1}{2}}\right\} \tag{A6a}$$

From equation (5) of the text,

$$F_2 = -\frac{\pi\beta}{M\alpha}(\Delta C_p)$$

$$= \frac{4\beta m}{M\sqrt{(m\beta - 1)(m\beta + 1)}} \tan^{-1}\left[\frac{2\beta m (v_w - v_0)}{M\epsilon (1 + \beta m)} - 1\right]^{-\frac{1}{2}} \tag{A7}$$

This function, which is equation (4) of the text, is shown in figure 8 for various values of θ_2 and $(v_w - v_0)/\epsilon$ for $M = \sqrt{2}$.

If the leading edge is curved, $Q(\epsilon) \neq 0$ and equation (A5) must be rearranged. The quantity in the radical may be expressed as

$$a' \left(1 - \frac{b'}{a'}\right)$$

where

$$a' = (c' + d'\epsilon)\epsilon = \left\{\left[2\beta^2 (y - \eta_0) - \frac{2 (x - \xi_0)}{m}\right] + \left(\frac{1}{m^2} - \beta^2\right)\epsilon\right\}\epsilon$$

$$b' = 2 (x - \xi_0) Q - 2 \left(\frac{\epsilon}{m}\right) Q - Q^2$$

$$c' = \frac{2 (x - \xi_0)(m\beta - 1)}{m}$$

$$d' = \frac{(1 - m^2 \beta^2)}{m^2} \qquad \text{(A8)}$$

Then equation (A5) may be written

$$- \frac{\pi}{2\alpha} (\Delta C_p) = \int_0^\epsilon \frac{d\epsilon}{\sqrt{a'} \sqrt{1 - \frac{b'}{a'}}}$$

Expanded in a power series,

$$\frac{1}{\sqrt{1 - \frac{b'}{a'}}} = 1 + \frac{1}{2} \frac{b'}{a'} + \frac{1}{2} \times \frac{3}{4} \left(\frac{b'}{a'}\right)^2 + \cdots$$

Equation (A5) then becomes

$$- \frac{\pi}{2\alpha} (\Delta C_p) = \int_0^\epsilon \frac{d\epsilon}{\sqrt{a'}} + \int_0^\epsilon \frac{\left[\frac{1}{2} \frac{b'}{a'} + \frac{1}{2} \times \frac{3}{4} \left(\frac{b'}{a'}\right)^2 + \cdots\right] d\epsilon}{\sqrt{a'}} \qquad \text{(A5a)}$$

The first term is identical with the integral of equation (A6). The contribution of the curvature to F_2 may therefore be written as

$$\Delta F_2 = \frac{2\beta}{M} \int_0^{\epsilon} \frac{\left[\frac{1}{2}\frac{b'}{a'} + \frac{1}{2}\times\frac{3}{4}\left(\frac{b'}{a'}\right)^2 + \cdots\right] d\epsilon}{\sqrt{a'}} \tag{A9}$$

The expressions for $\frac{b'}{a'}$ and $\frac{1}{\sqrt{a'}}$ in equation (A8) may be expanded in a power series to yield

$$\frac{b'}{a'} = \frac{2}{c'}\left\{\left[(x - \xi_0)a_2\right]\epsilon + \left[(x - \xi_0)a_3 - \frac{a_2}{m} - \frac{d'}{c'}(x - \xi_0)a_2\right]\epsilon^2 + \left[(x - \xi_0)a_4 - \frac{2a_3}{m}a_2^2 - \left(\frac{d'}{c'}\right)(x - \xi_0)a_3 + \left(\frac{d'}{c'}\right)\frac{a_2}{m} + \left(\frac{d'}{c'}\right)^2 (x - \xi_0)a_2\right]\epsilon^3 + \cdots\right\}$$

$$\frac{1}{\sqrt{a'}} = \frac{1}{\sqrt{\epsilon}} \frac{1}{\sqrt{c'\left(1 + \frac{d'}{c'}\epsilon\right)}}$$

$$= \frac{1}{\sqrt{\epsilon}} \frac{1}{\sqrt{c'}} \left[1 - \frac{1}{2}\left(\frac{d'}{c'}\right)\epsilon + \frac{1}{2}\times\frac{3}{4}\left(\frac{d'}{c'}\right)^2\epsilon^2 - \frac{1}{2}\times\frac{3}{4}\times\frac{5}{6}\left(\frac{d'}{c'}\right)^3\epsilon^3 + \cdots\right]$$

where

$$\frac{d'}{c'} = \frac{-(1 + m\beta)}{2m(x - \xi_0)} \tag{A10}$$

Upon substitution of equation (A10) in equation (A9) and multiplication and collection of terms according to powers of ϵ, there results

$$\Delta F_2 = \frac{2\beta}{M}\left(\frac{1}{c'}\right)^{\frac{3}{2}}\int_0^{\epsilon}\left(3C_1\epsilon^{\frac{1}{2}} + 5C_2\epsilon^{\frac{3}{2}} + 7C_3\epsilon^{\frac{5}{2}} + \cdots\right)d\epsilon$$

$$= \frac{4\beta}{M}\left(\frac{1}{c'}\right)^{\frac{3}{2}}\left(C_1\epsilon^{\frac{3}{2}} + C_2\epsilon^{\frac{5}{2}} + C_3\epsilon^{\frac{7}{2}} + \cdots\right) \qquad \text{(A9a)}$$

where

$$C_1 = \frac{1}{3}(x - \xi_0)a_2$$

$$C_2 = \frac{1}{5}\left\{\frac{(3\beta m - 1)a_2}{4m} + \left[a_3 + \frac{3a_2{}^2 m}{4(\beta m - 1)}\right](x - \xi_0)\right\}$$

$$C_3 = \frac{1}{7}\left\{\frac{3(\beta m + 1)(5\beta m - 3)a_2}{32m^2(x - \xi_0)} + \frac{(7\beta m - 1)a_2{}^2}{16(\beta m - 1)} + \frac{(3\beta m - 1)a_3}{4m}\right.$$

$$\left. + \left[a_4 + \frac{3a_2a_3m}{2(\beta m - 1)} + \frac{5a_2{}^3m^2}{8(\beta m - 1)^2}\right](x - \xi_0)\right\} \qquad \text{(A11)}$$

$$C_4 = \cdots$$

The series of equation (A9a) converges as long as b'/a' and $d'\epsilon/c'$ (defined by equations (A8) and (A10)) are less than unity. For rapid convergence, these ratios should both be small.

As a particular example (taken at $M = \sqrt{2}$), the leading-edge curve may be represented by the parabola

$$\xi = \xi_0 + \frac{\epsilon}{m} + a_2\epsilon^2$$

The coefficients of equation (A11) evaluated in terms of the oblique coordinate distances then become

$$C_1 = \frac{\sqrt{2}}{6}(v_w - v_0)a_2$$

$$C_2 = \frac{1}{5}\left[\frac{(3m - 1)a_2}{4m} + \frac{3\sqrt{2}\, a_2^2 m(v_w - v_0)}{8(m - 1)}\right]$$

$$C_3 = \frac{1}{7}\left[\frac{3\sqrt{2}(m + 1)(5m - 3)a_2}{32m^2\,(v_w - v_0)} + \frac{(7m - 1)a_2^2}{16(m - 1)} + \frac{5\sqrt{2}\, a_2^3 m^2(v_w - v_0)}{16(m - 1)^2}\right]$$

$C_4 = \cdots$

When the values of the coefficients are substituted in equation (A9a), ΔF_2 results.

For a parabola with a given initial slope m at the point (ξ_0, η_0), the quantity a_2 controls the radius of curvature r_0 at that point. The ratio $\Delta F_2/F_2$ represents the relative error resulting from the assumption of a straight leading edge for a width ϵ when the actual edge is curved. This value from equations (A7) and (A9a) has been plotted against the ratio ϵ/r_0 in figure 12.

APPENDIX B

TREATMENT OF COMPLETE WINGS

A tabular summation of the various flow fields encountered in wing problems is presented in table II and the graphical solution in each region is indicated. In the reference sketches for $M = \sqrt{2}$, P is the point at which the pressure coefficient is to be evaluated. The numerical line integration along the supersonic leading edge is performed from point a to point b. The direction of integration of the line integrals is indicated by arrowheads on heavy lines. For a subsonic trailing edge (sketches C, F, G, H), the Kutta-Joukowski condition was imposed and made $F_1 = 0$ for that edge. The factor F_2 vanishes when the limit of the leading-edge line integral is other than the integration-grid edge (sketches D, E, F, G, H), because no infinities are then encountered. When the forward-reflected Mach lines from the point P cross on the wing surface (sketches E, F), the integration H is considered negative.

The occurrence of these flow fields on a schematic wing is illustrated in figure 15. Each flow region is identified by the corresponding letter from table II. In this example, flow region H does not occur.

As an example of the method, numerical calculations of the pressure coefficient at point P for the wing boundary shown in figure 10 are

$$\left.\begin{aligned} \theta_1 &= 7.5^\circ \\ \overline{bc} &= 0.0419 \\ \overline{cd} &= 0.084 \\ R &= \frac{\overline{bc}}{\overline{cd}} = 0.4988 \end{aligned}\right\} \quad F_1 = 0.224$$

$$\left.\begin{aligned} \theta_2 &= 125.5^\circ \\ (v_w - v_0) &= 0.0772 \\ \epsilon &= 0.01 \end{aligned}\right\} \qquad F_2 = 0.660$$

$$H = 0.01\,[(0.4)(31) + 25.0 + 21.0 + 18.85 + 17.55 + 16.75 + 16.50 + 16.6] = 1.446$$

$$-\frac{C_p}{\alpha} = +\frac{\sqrt{2}}{\pi}(H + F_1 + F_2) = 1.048$$

APPENDIX C

SIMPLIFYING CONSIDERATIONS IN APPLICATION OF METHOD

A simple method of obtaining coordinates of hyperbolas to construct an integration grid employs log-log graph paper. If a straight line of slope equal to -1 is drawn on this paper, the coordinates of this line, when plotted in Cartesian coordinates, describe the desired equilateral hyperbola.

The addition to the grid of lines of constant v and u (parallel to the grid edges) with accompanying scales at the grid edges increases the rapidity of evaluation, because all significant distances may then be read directly. A part of the grid employed is given in figure 7.

In choosing the value of ϵ, the first consideration is that ϵ be large enough that the value of h may be easily determined for the first subsequent element. It is also seen from figure 8 that if ϵ is taken as a simple decimal such as 0.01 or 0.02, and $(v_w - v_0)$ is known, the ratio $(v_w - v_0)/\epsilon$ may be rapidly computed and hence F_2 is rapidly determined. From figure 6, point a will not, in general, fall at an integral multiple of $\Delta\eta$; then, if $\epsilon = N\Delta\eta$ where N is an integer, point a' will not, in general, fall on an integral multiple of $\Delta\eta$. Thus a section whose width is less than $\Delta\eta$ appears before the first complete leading-edge element and remains to be included in the numerical integration. If this small element is evaluated in the normal manner and weighted according to its width, no discrepancy will occur. This weighting process is illustrated by the example presented in appendix B.

The most prevalent personal error in the application of the method was in the measurement of angles θ_1 and θ_2, because on small drawings it is difficult to judge accurately the tangency of a curve. Large-scale drawings are therefore recommended for measuring the angles. These drawings may also be used for the integration, although the increase in accuracy may not justify the accompanying inconvenience.

For a straight supersonic leading edge, equation (1) is integrable and the expression for C_p becomes

$$C_p = -\frac{2\alpha}{\pi\beta}\left[\left(1 - \frac{du_2}{dv_w}\right)\sqrt{\frac{v_w + k_1 u_2}{u_w - u_2}} + \frac{k_1 + 1}{\sqrt{k_1}} \tan^{-1}\sqrt{\frac{k_1(u_w - u_2)}{v_w + k_1 u_2}}\right] \quad (C1)$$

In the region affected by the subsonic trailing edge (region abc of figs. 16 and 17) the first term in equation (C1) vanishes if the Kutta-Joukowski condition is imposed. The quantity in the radical of the arc-tangent term is proportional to the ratio of distances $\overline{sP}/\overline{rs}$ (fig. 16) and hence any wing composed of the same leading edge and a straight line through point s would give the same value of C_p for any point on line $\overline{sP}$. If lines of constant pressure are desired, the arc-tangent term in equation (C1) must be differentiated and set equal to zero. The result involves a derivative du_2/dv_w, which is determined by the slope of the edge at point s. Equivalent lines of constant pressure along line $\overline{sP}$ may thus be obtained by replacing the tip by a straight-line tip that is tangent at point s. The pressure along any v = constant line is therefore conical about a point determined by the intersection of the extension of the leading edge and the tangent to the tip at $u_2(v_w)$. Along $v = v_1$ and $v = v_2$ (fig. 17), the constant-pressure lines are conical about points t_1 and t_2. By this relation, the constant-pressure lines may be quickly constructed and evaluation is necessary only along one line of constant x to determine the pressure field. The relation holds only in the region influenced by the subsonic trailing edge when the Kutta-Joukowski condition applies, for differentiation of equation (C1) with the first term included yields a second derivative that generally cannot be evaluated from straight-line relations.

REFERENCES

1. Evvard, John C.: Distribution of Wave Drag and Lift in the Vicinity of Wing Tips at Supersonic Speeds. NACA TN No. 1382, 1947.

2. Evvard, John C.: Theoretical Distribution of Lift on Thin Wings at Supersonic Speeds (An Extension). NACA TN No. 1585, 1948.

TABLE I

VALUES OF C_p/α OBTAINED FOR WINGS A AND B

Station	u	v	Wing A			Wing B		
			C_p/α		Error (percent)	C_p/α		Error (percent)
			Analytic	Graphic		Analytic	Graphic	
1	8	0	2.4570	2.468	0.44	2.457	2.447	0.16
2	7	1	2.1354	2.148	.59	1.866	1.875	.48
3	6	2	1.9826	1.975	.38	1.674	1.679	.30
4	5	3	1.8577	1.871	.71	1.578	1.584	.38
5	4	4	1.7861	1.775	.62	1.744	1.733	.63
6	3	5	2.3877	2.400	.52			
7	8	2	2.0395	2.033	.32	1.775	1.759	.90
8	7	3	1.9295	1.933	.18	1.689	1.682	.41
9	6	4	1.8367	1.827	.53	1.676	1.670	.36
10	5	5	1.7861	1.797	.61	1.862	1.865	.16
11	4	6	2.0147	2.012	.13			
Average					0.46			0.42

TABLE II - PRESSURE COEFFICIENT FOR EACH WING REGION

Type of region	Reference figure	Pressure coefficient	Special features
A	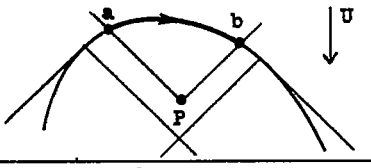	$C_p = \frac{M\alpha}{\pi\beta}\left[H + F_2 + F_{2,r}\right]$	Affected only by supersonic leading edge.
B	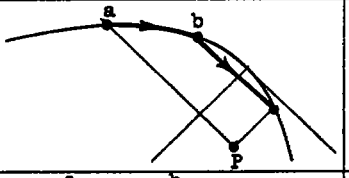	$C_p = \frac{M\alpha}{\pi\beta}\left[H + F_1 + F_2\right]$	Affected by subsonic and supersonic leading edges.
C	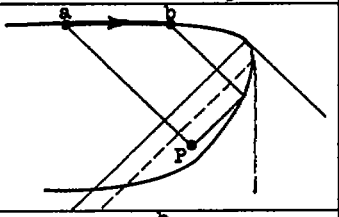	$C_p = \frac{M\alpha}{\pi\beta}\left[H + F_2\right]$	Affected by subsonic trailing and supersonic leading edges. Kutta-Joukowski condition imposed. $F_1 = 0$.
D	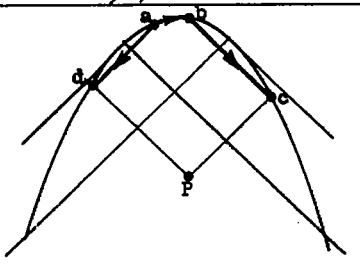	$C_p = \frac{M\alpha}{\pi\beta}\left[H + F_1 + F_{1,l}\right]$	Affected by supersonic and both subsonic leading edges. $F_{1,l}$ found for strip $\overline{ad}$ in same manner as F_1 for strip $\overline{bc}$. For $F_{1,l}$ use $R_l = \frac{\overline{ad}}{\overline{df}}$ and measure $\theta_{1,l}$ clockwise at point d.
E	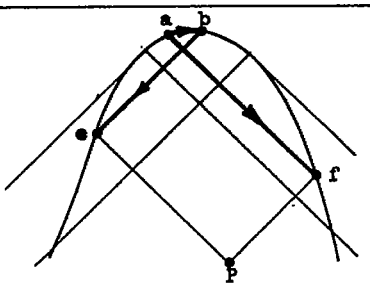	$C_p = \frac{M\alpha}{\pi\beta}\left[-H + F_1 + F_{1,l}\right]$	Affected by supersonic and both subsonic leading edges. $F_{1,l}$ determined as for region D with $R_l = \frac{\overline{be}}{\overline{ef}}$.

NACA

TABLE II - PRESSURE COEFFICIENT FOR EACH WING REGION - Concluded

Type of region	Reference figure	Pressure coefficient	Special features
F	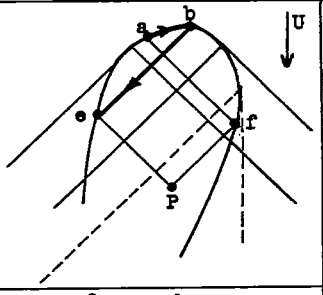	$C_p = \frac{M\alpha}{\pi\beta}\left[-H + F_{1,l}\right]$	Affected by one subsonic leading and one subsonic trailing edge. $F_{1,l}$ determined as previously with $R_l = \frac{\overline{be}}{\overline{eF}}$. Kutta-Jowkowski condition imposed on subsonic trailing edge. $F_1 = 0$.
G	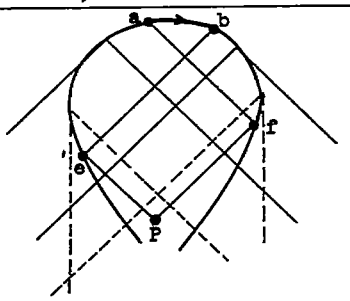	$C_p = \frac{M\alpha}{\pi\beta}\left[-H\right]$	Affected by both subsonic trailing edges. Kutta-Joukowski condition imposed. $F_1 = F_{1,l} = 0$.
H	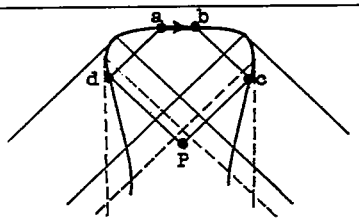	$C_p = \frac{M\alpha}{\pi\beta}\left[H\right]$	Affected by both subsonic trailing edges. Kutta-Joukowski condition imposed. $F_1 = F_{1,l} = 0$.
I	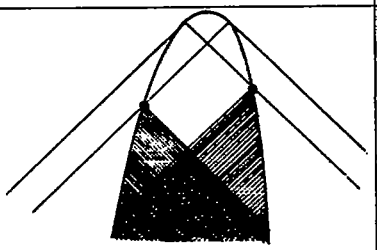		Shaded region is affected by externally interacting flow fields. Solution not handled by graphical method.

NACA

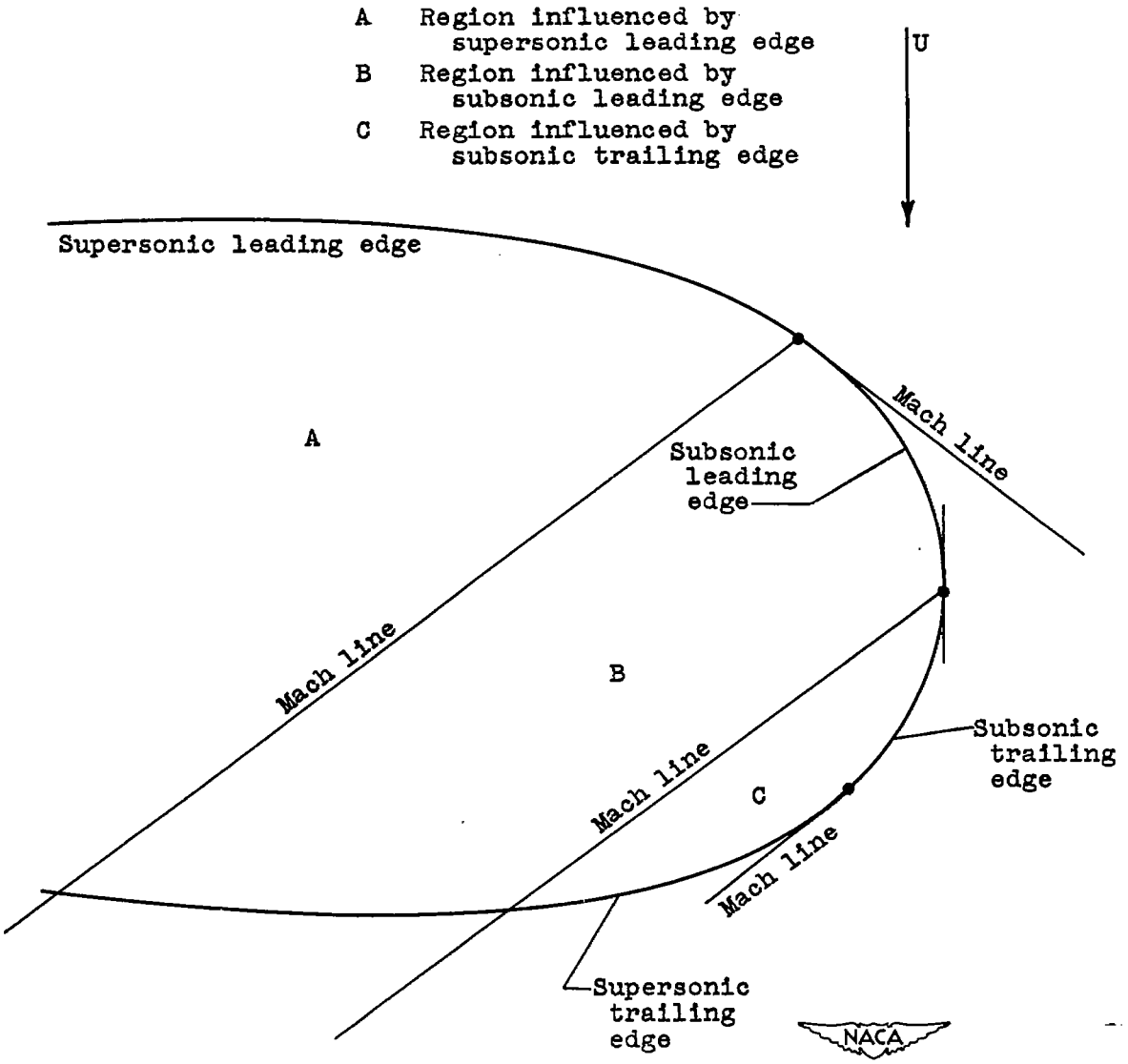

Figure 1. - Illustration of wing regions.

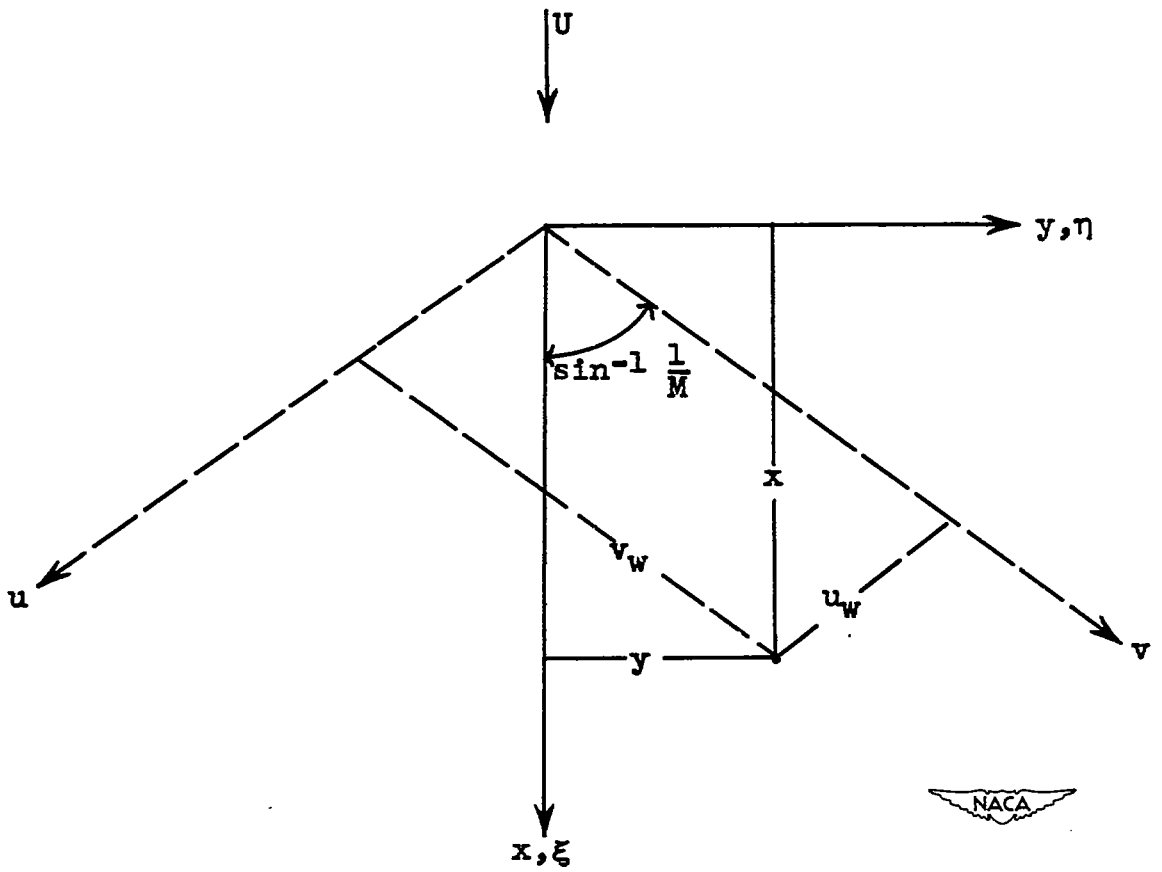

Figure 2. - Relation between oblique and Cartesian coordinates.

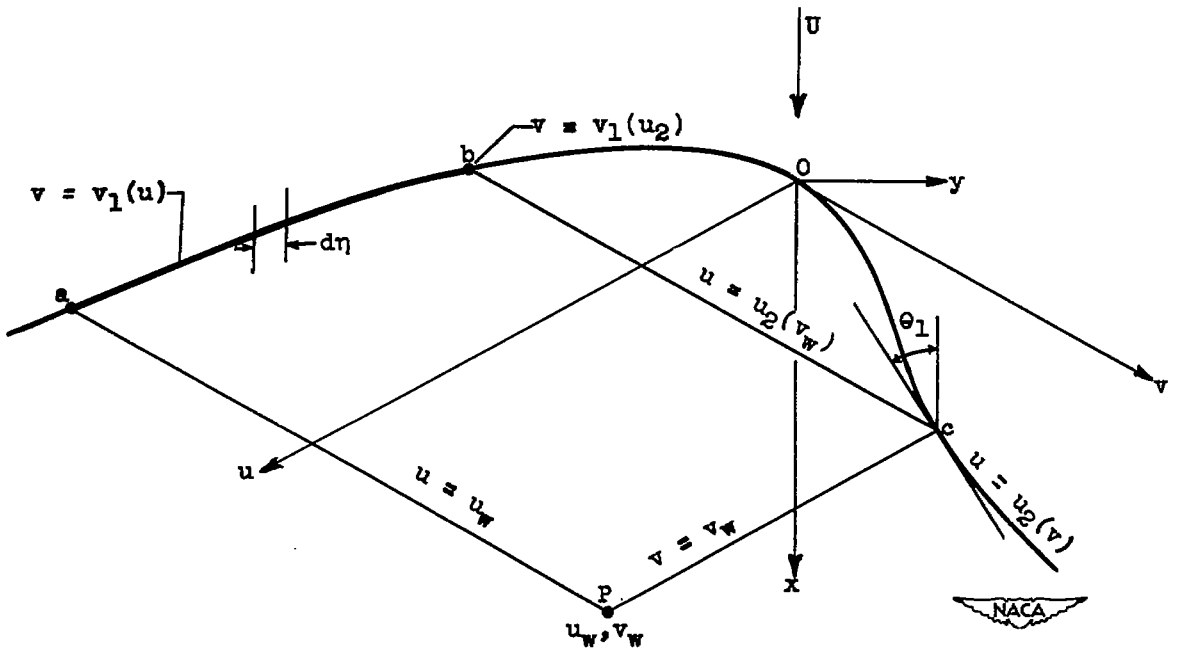

Figure 3. - Geometric interpretation of terms in equation (1).

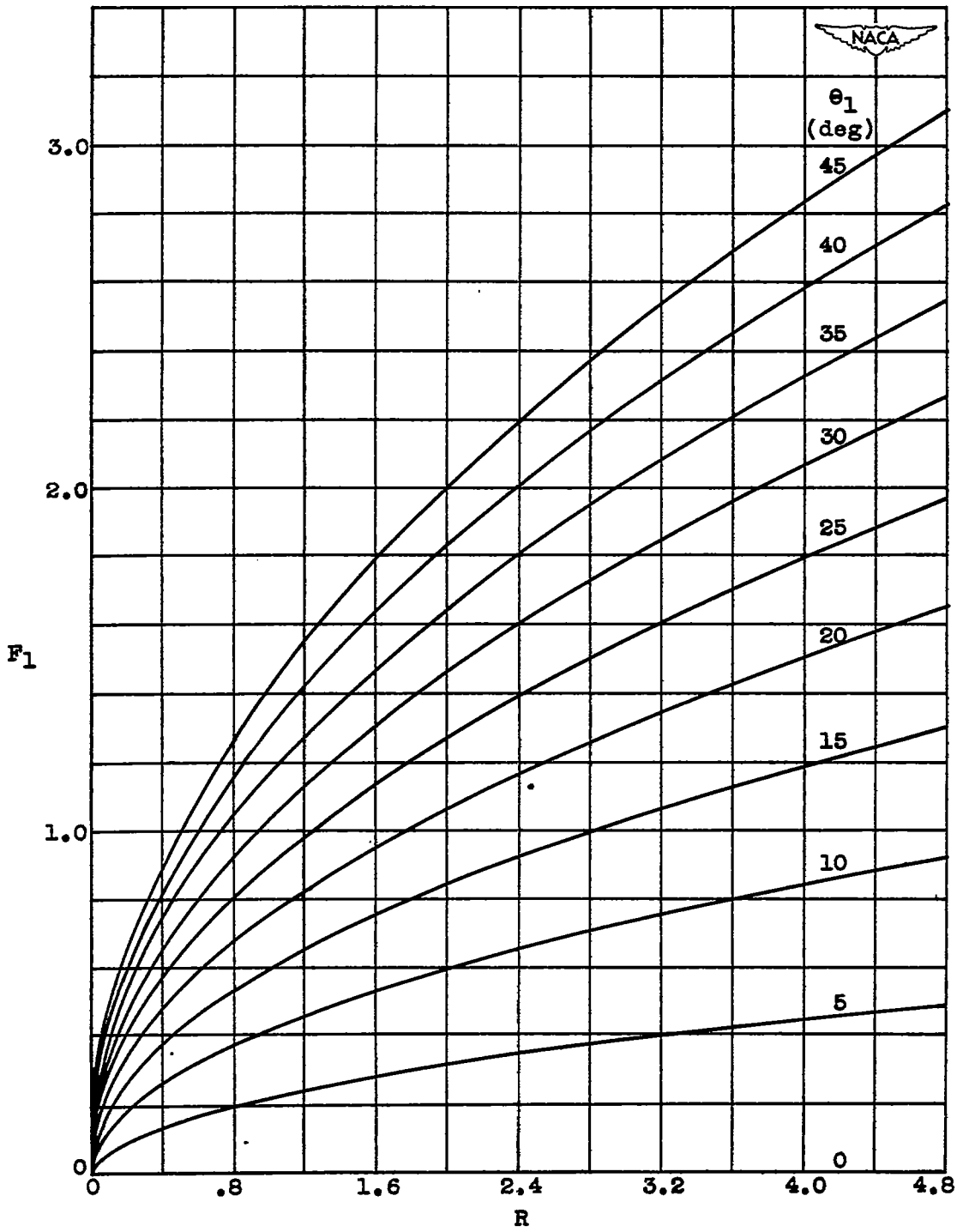

(a) Range of R from 0 to 4.8.

Figure 4. - Variation of factor F_1 with R and θ_1 for $M = \sqrt{2}$.

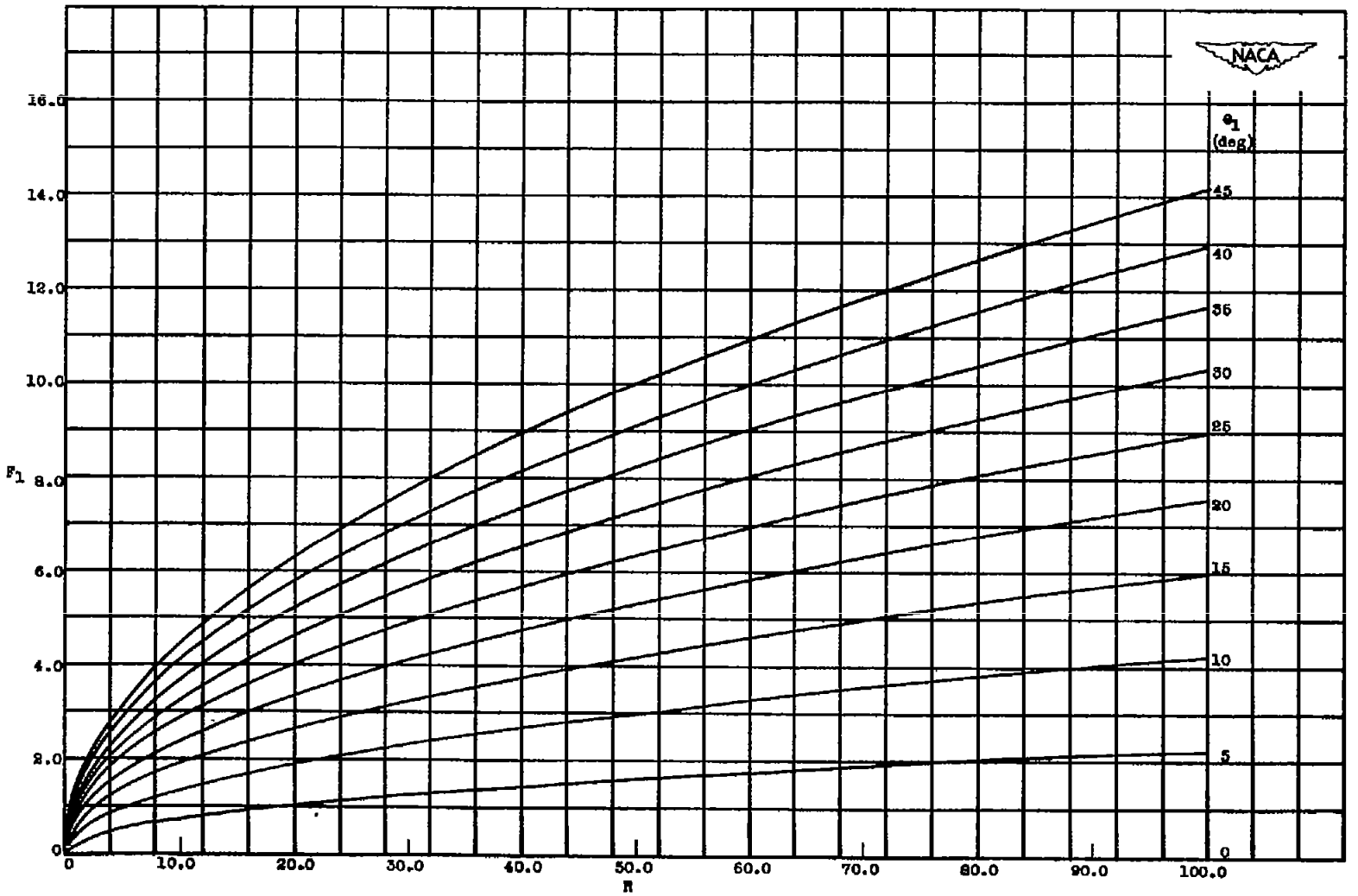

(b) Range of R from 0 to 100.

Figure 4. - Concluded. Variation of factor F_1 with R and θ_1 for $M = \sqrt{2}$.

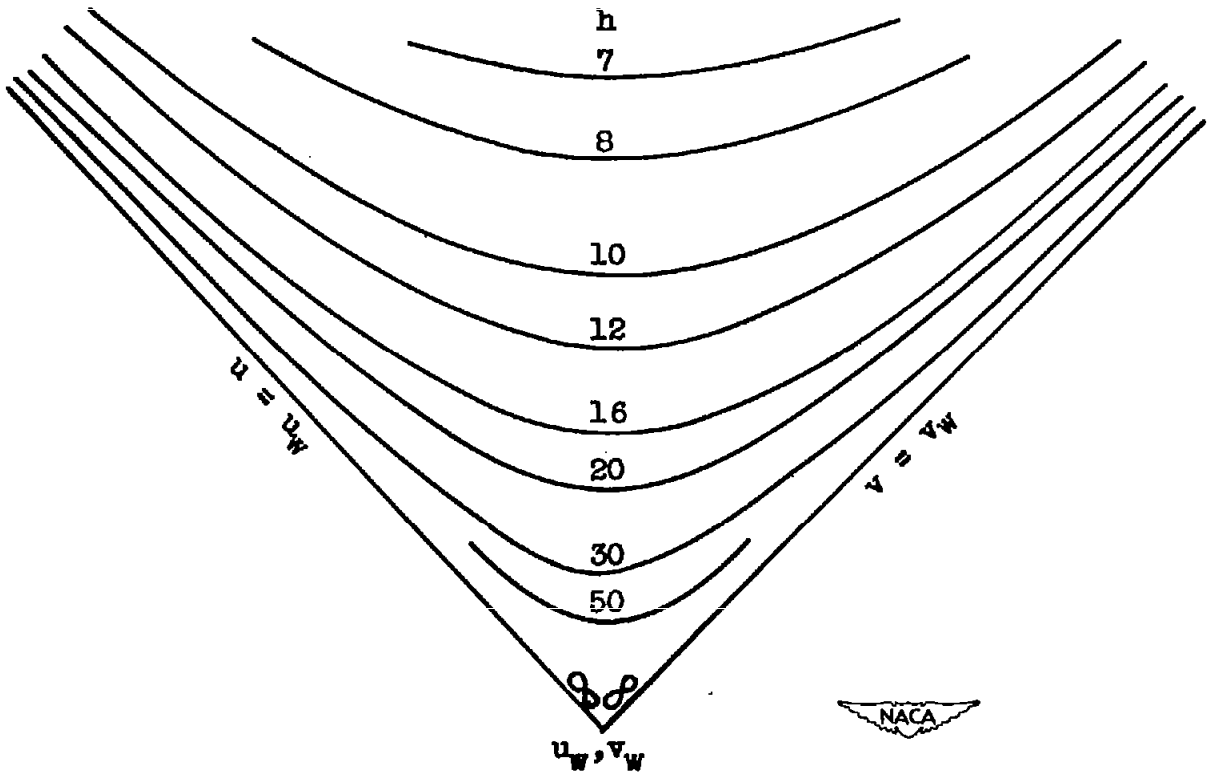

Figure 5. - Schematic hyperbolic integration grid.

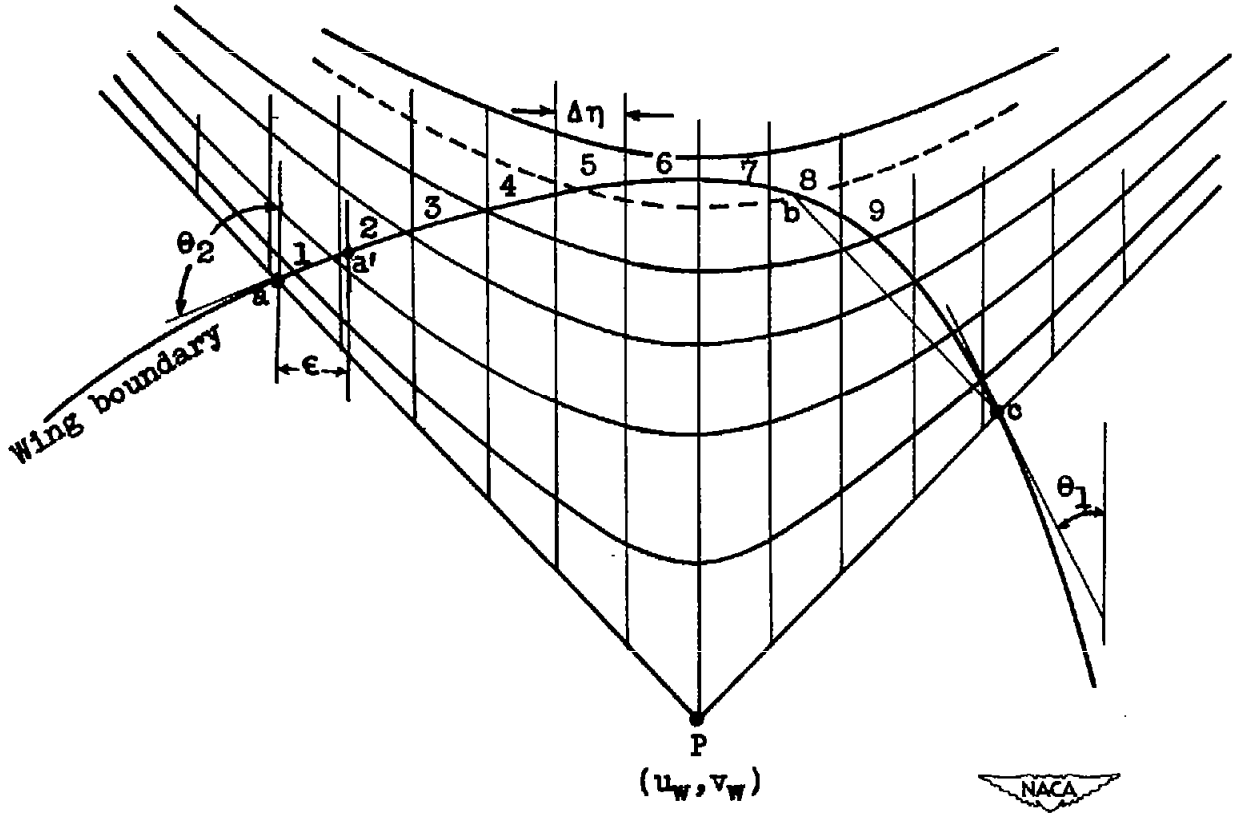

Figure 6. - Schematic illustration of wing boundary superimposed on integration grid. $M = \sqrt{2}$.

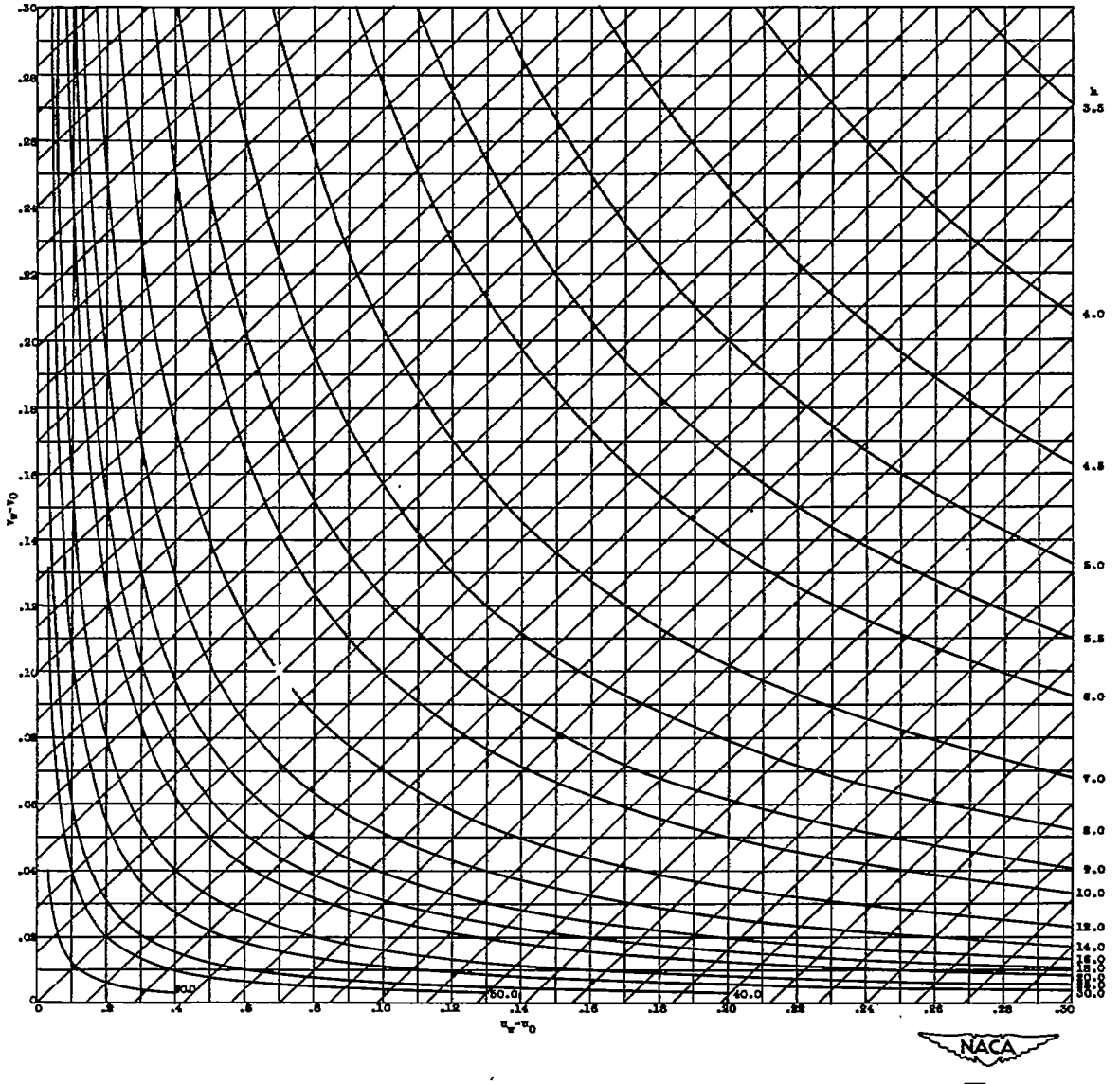

Figure 7. - Part of integration grid employed for calculations at $M = \sqrt{2}$.

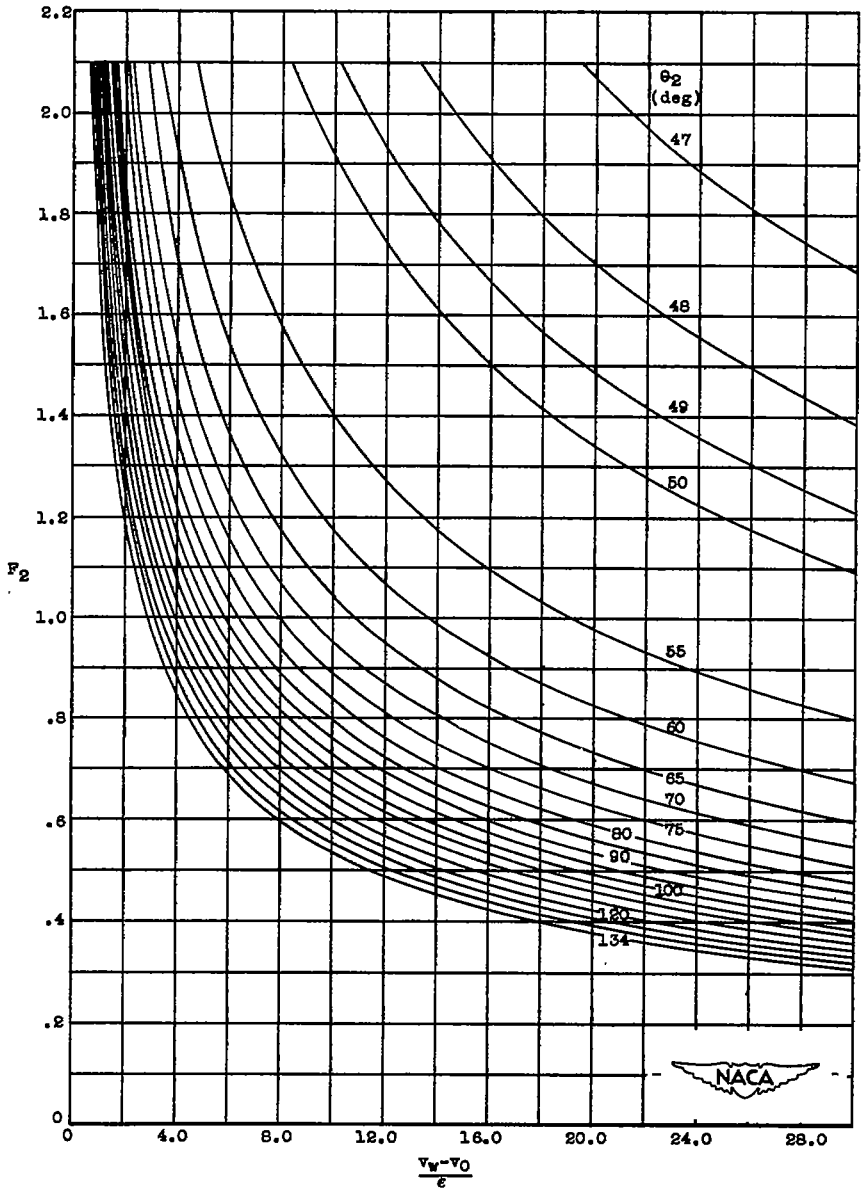

(a) Range of F_2 from 0 to 2.1.

Figure 8. - Variation of factor F_2 with $\frac{(V_w-V_0)}{\epsilon}$ for various values of θ_2 at $M = \sqrt{2}$.

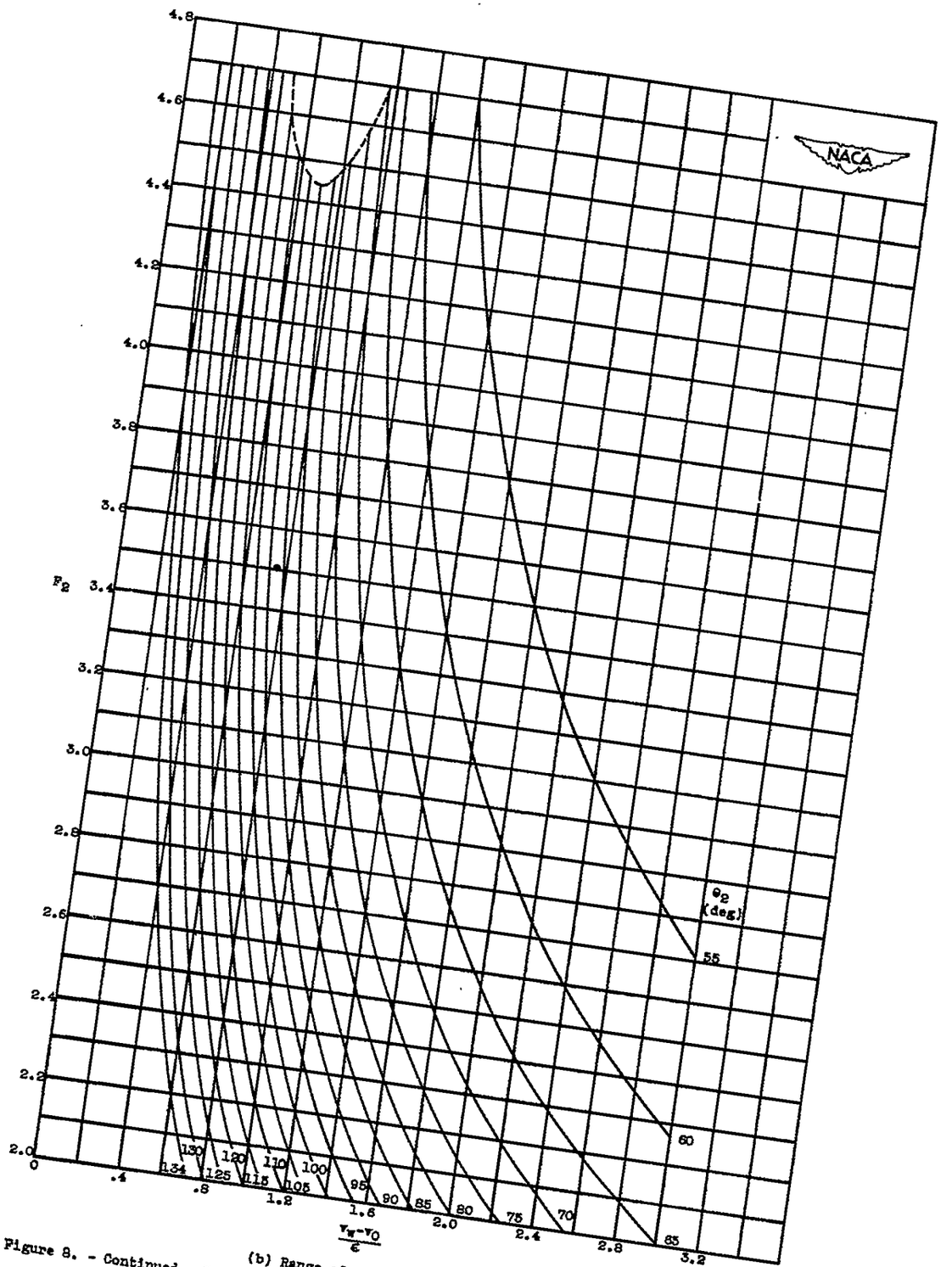

Figure 8. - Continued. Variation of factor F_2 with $(V_w-V_0)/\epsilon$ for various values of θ_2 at $M = \sqrt{2}$.

(b) Range of F_2 from 2.0 to 4.7.

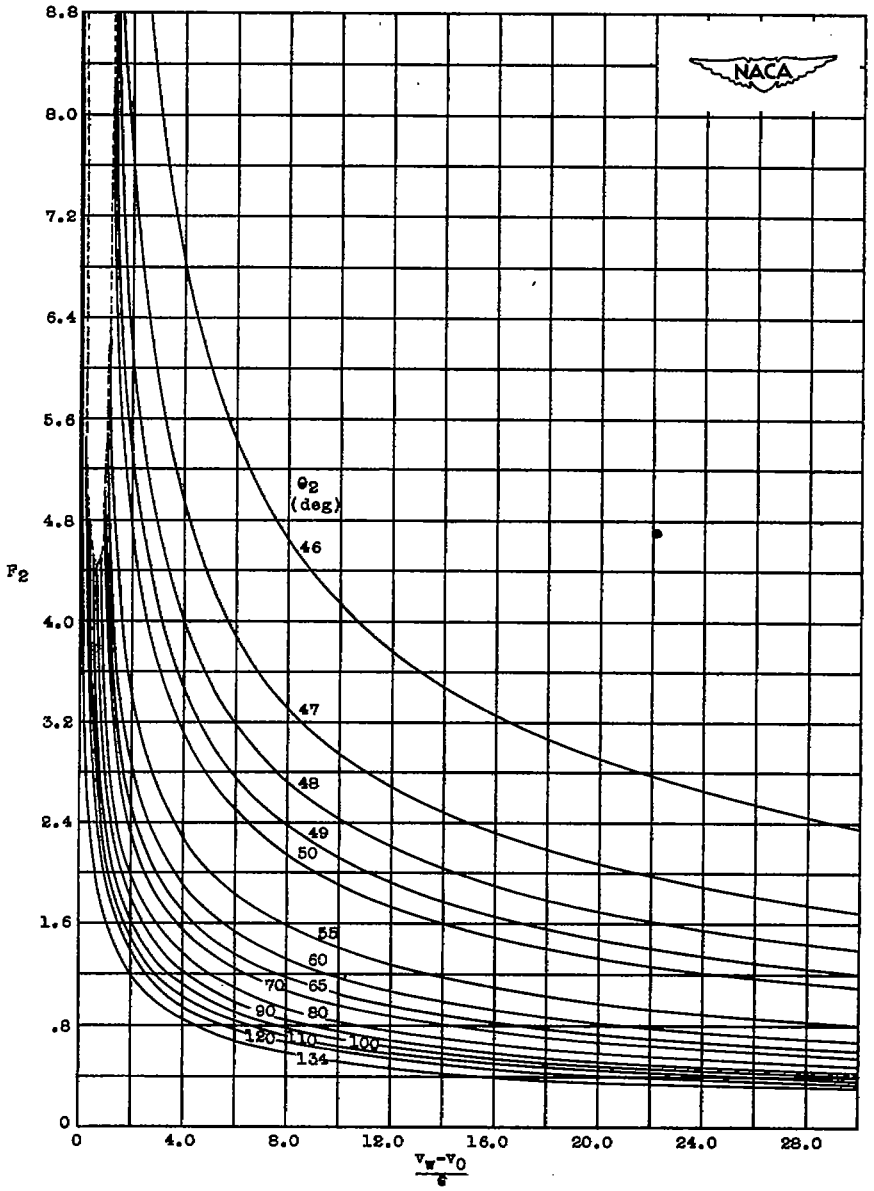

(c) Range of F_2 from 0 to 8.8.

Figure 8. - Concluded. Variation of factor F_2 with $(v_w-v_0)/\epsilon$ for various values of θ_2 at $M = \sqrt{2}$.

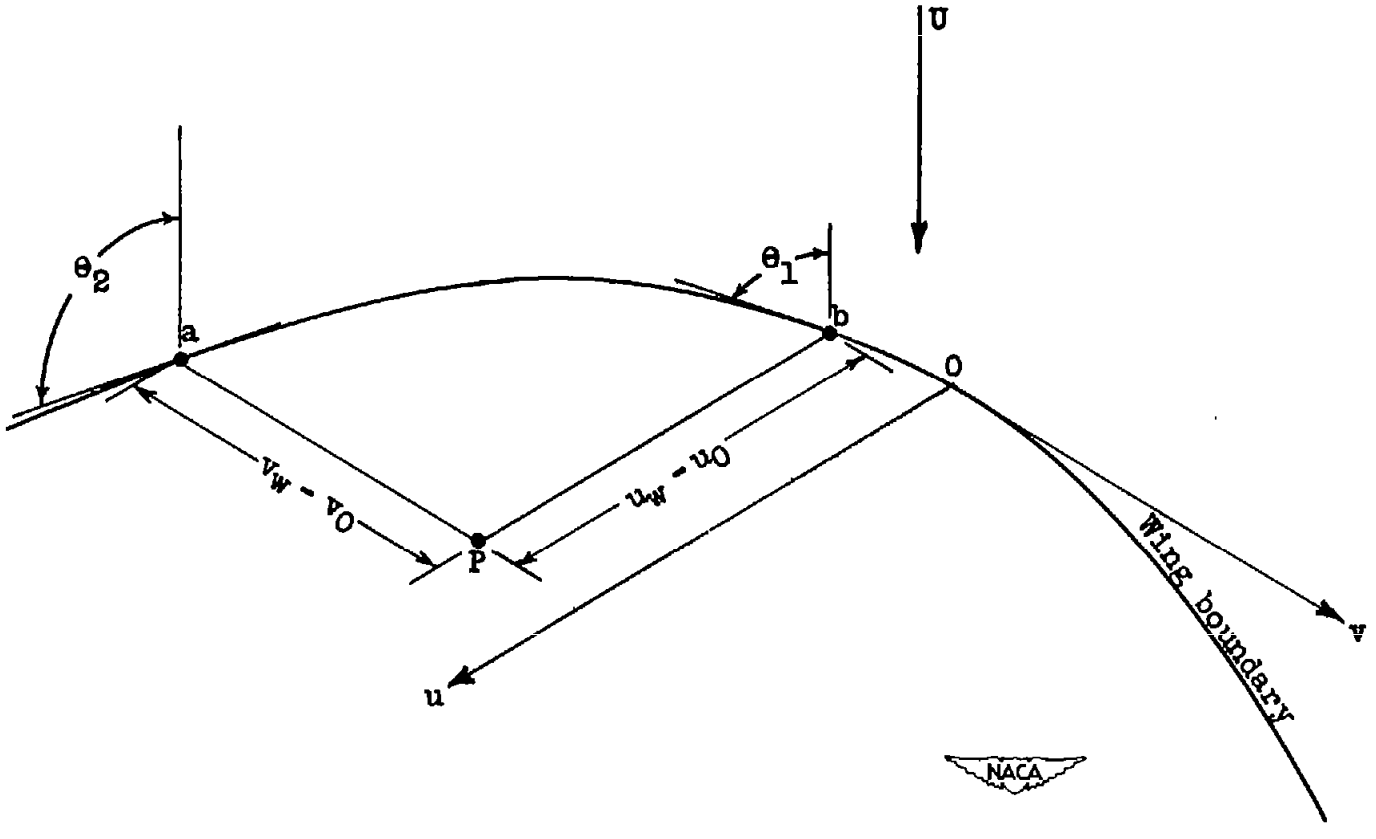

Figure 9. - Parameters in region A ($v < 0$).

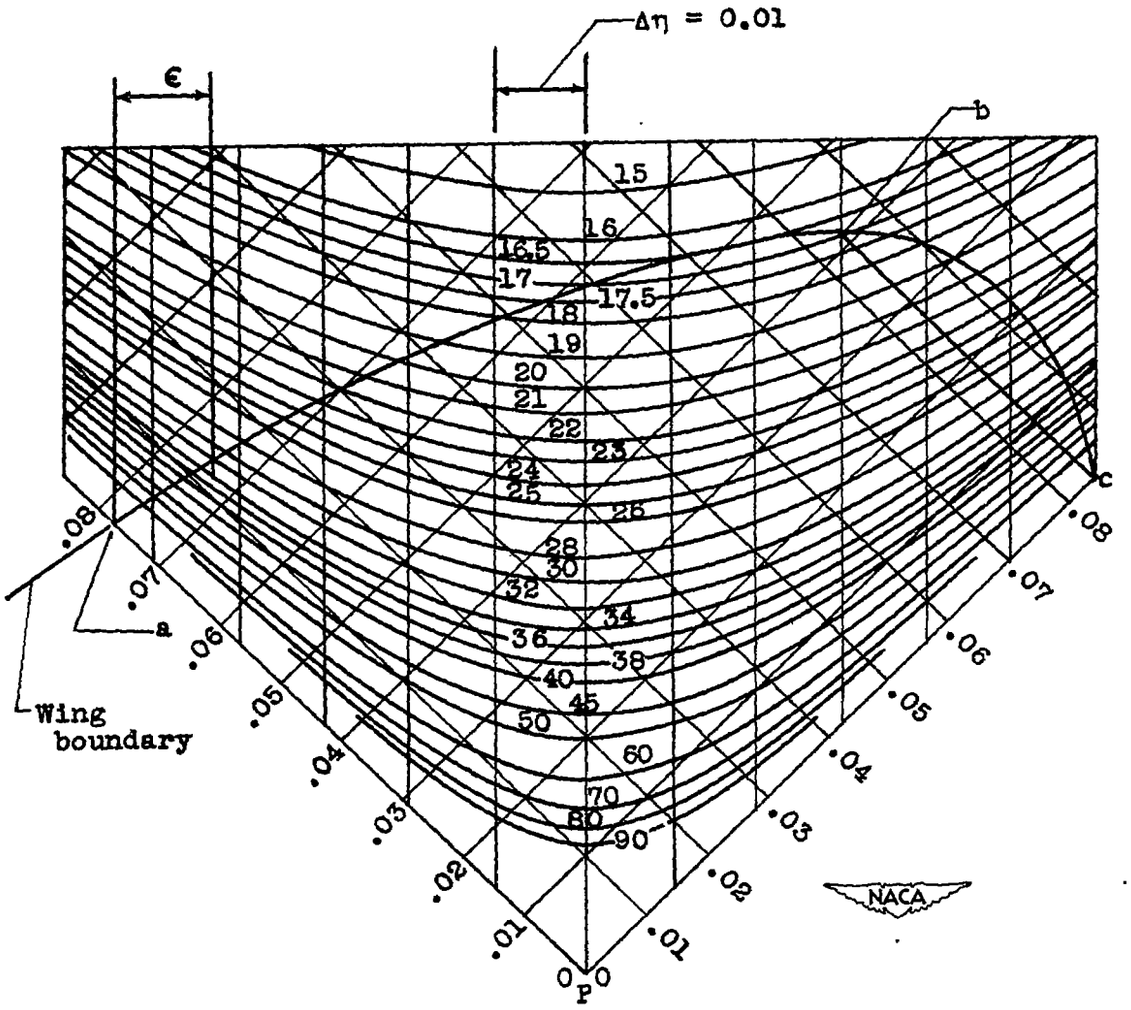

Figure 10. - Determination of C_p for specific wing boundary at $M = \sqrt{2}$.

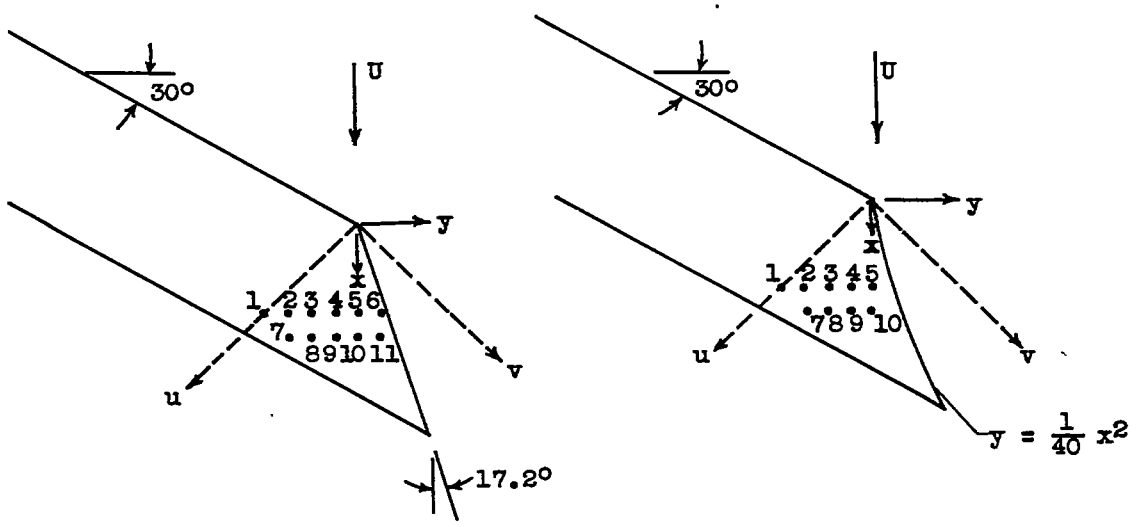

(a) Wing A. (b) Wing B.

Figure 11. - Wings used for comparison of graphical and closed-form solutions.

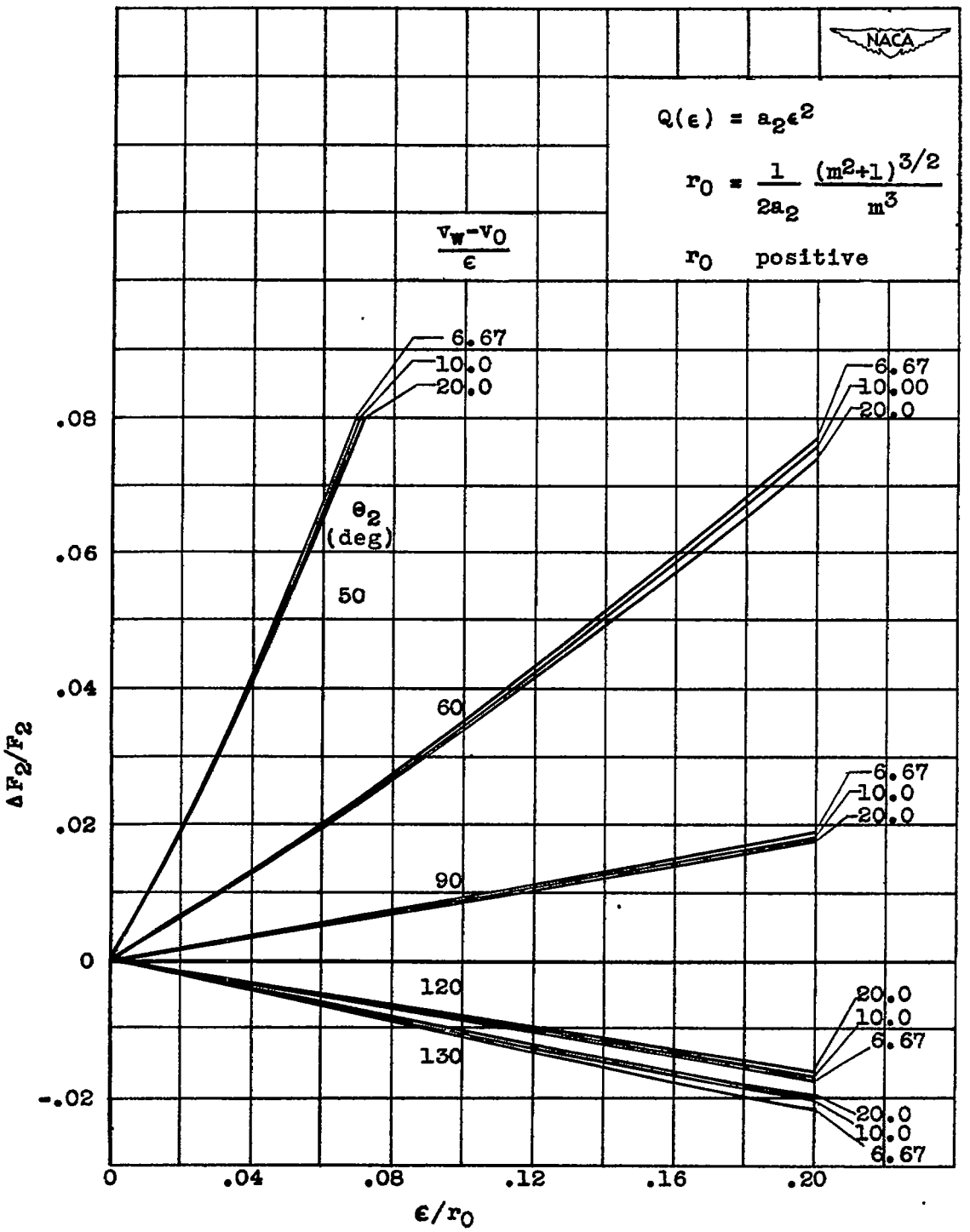

Figure 12. - Effect of curvature on factor F_2 at $M = \sqrt{2}$.

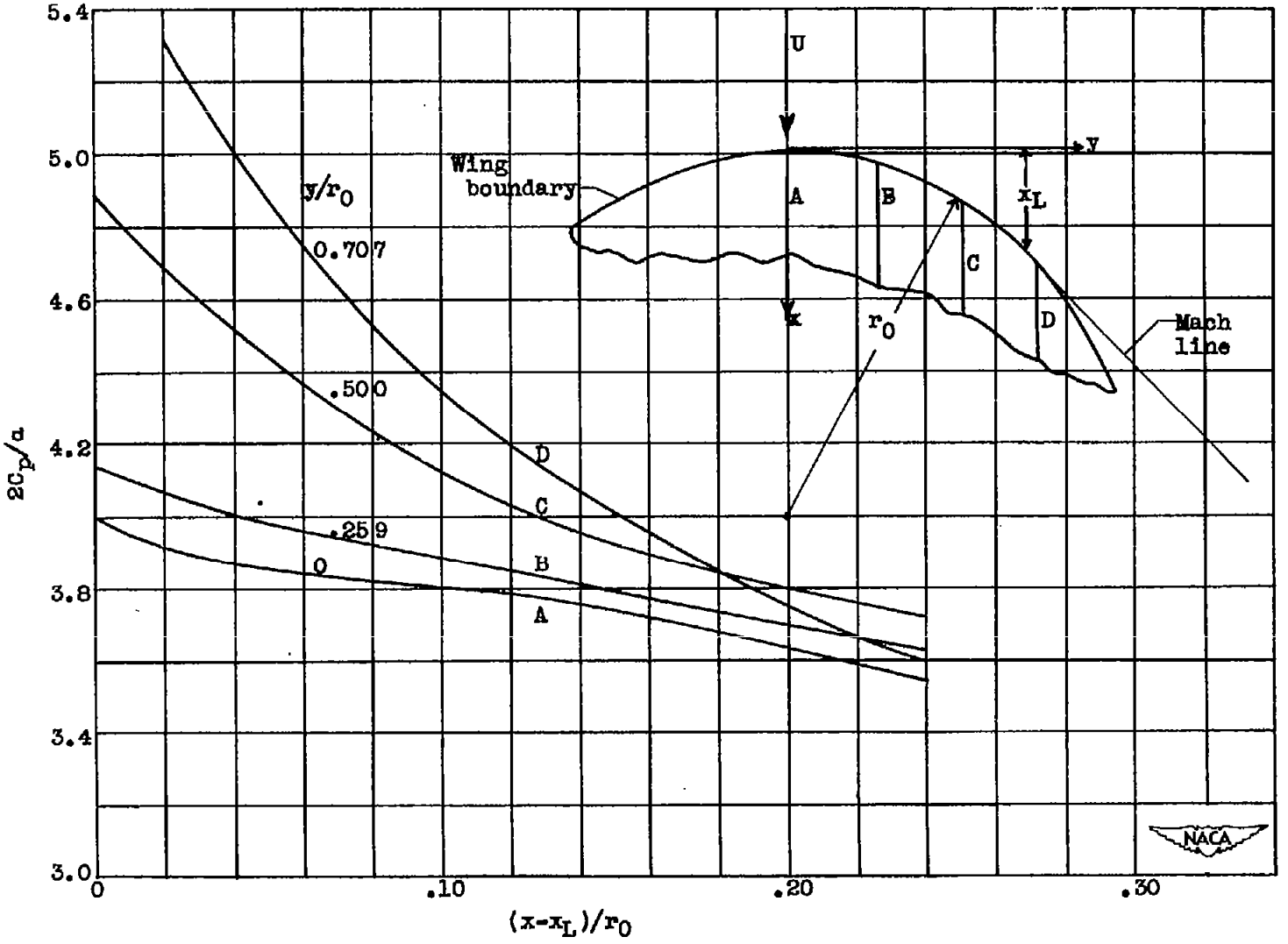

Figure 13. - Lift distribution on thin circular-plan-form wing at $M = \sqrt{2}$.

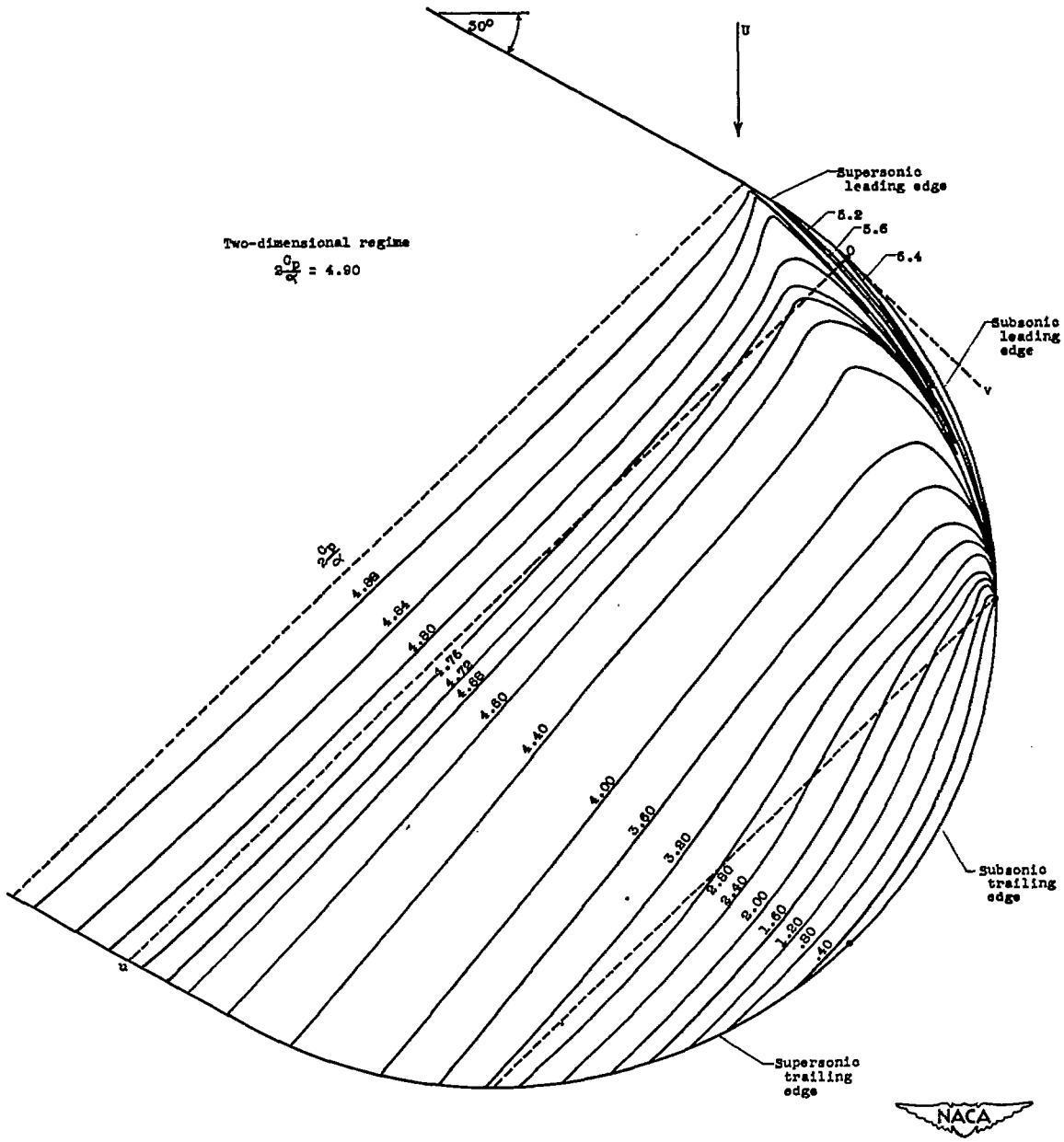

Figure 14.- Lift distribution for $M = \sqrt{2}$ on circular-tip wing swept back at 30°. $2\frac{c_p}{\alpha}$ on subsonic leading edge = ∞, on subsonic trailing edge = 0.

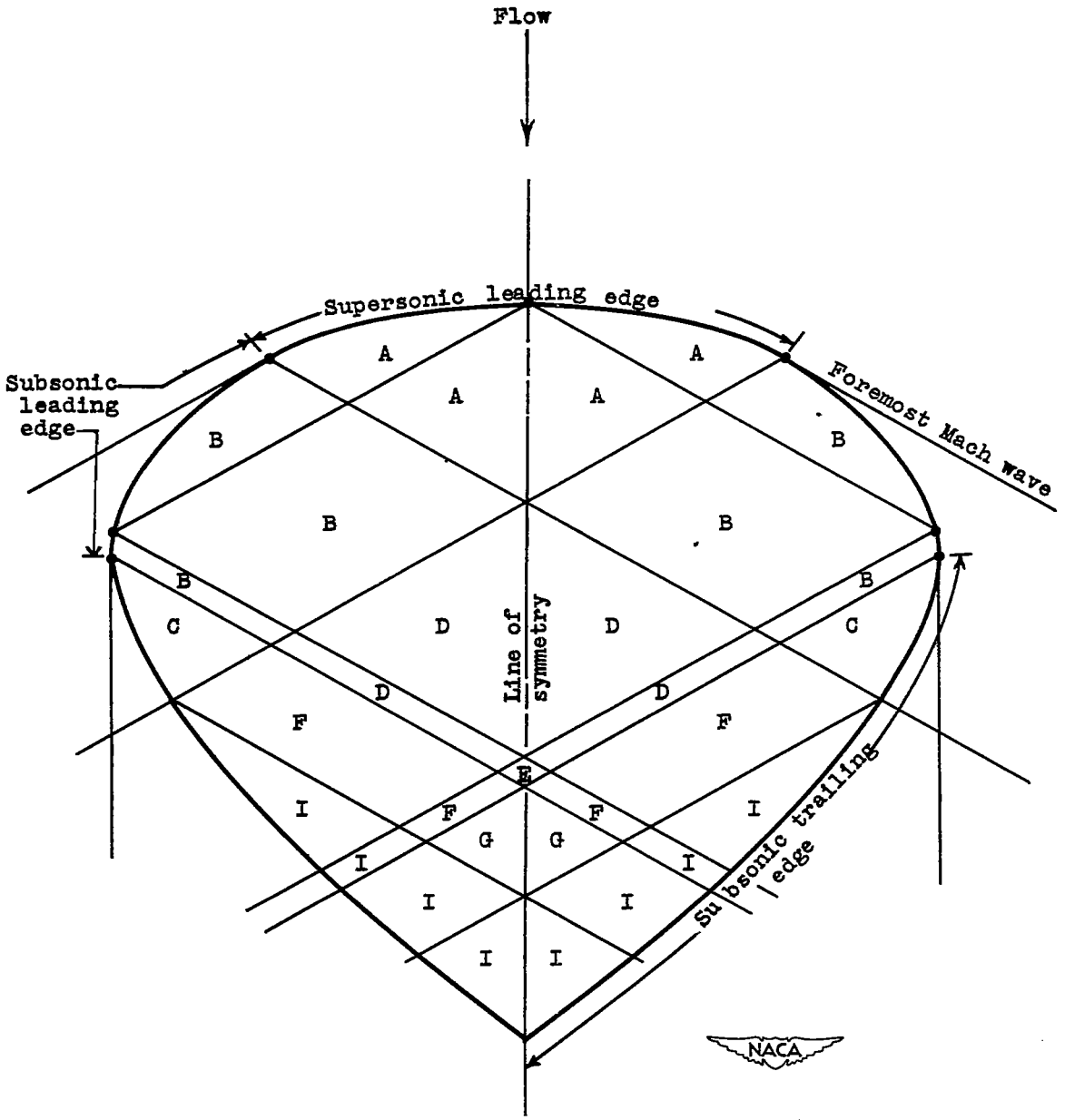

Figure 15. - Wing illustrating regions considered in table II.

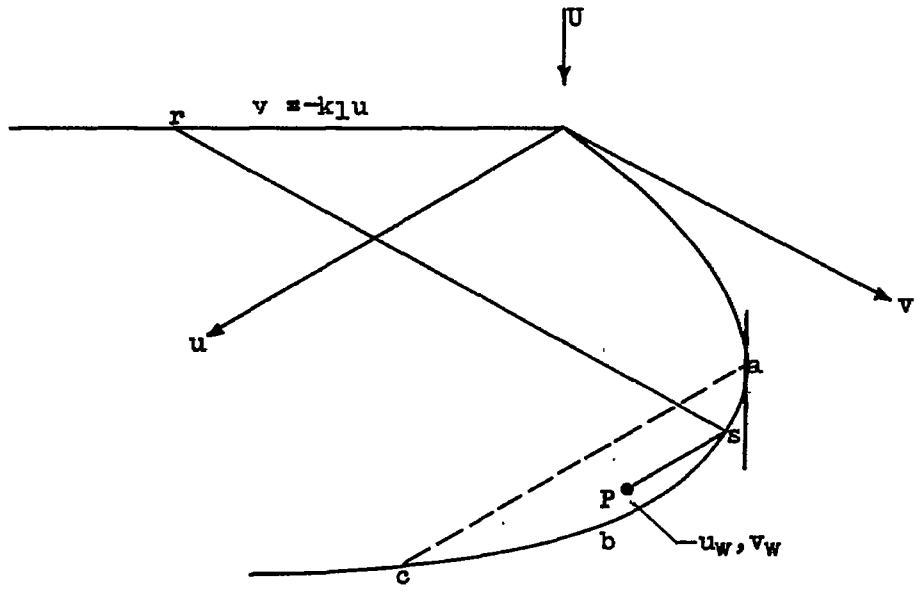

Figure 16. - Wing with subsonic trailing edge and straight supersonic leading edge.

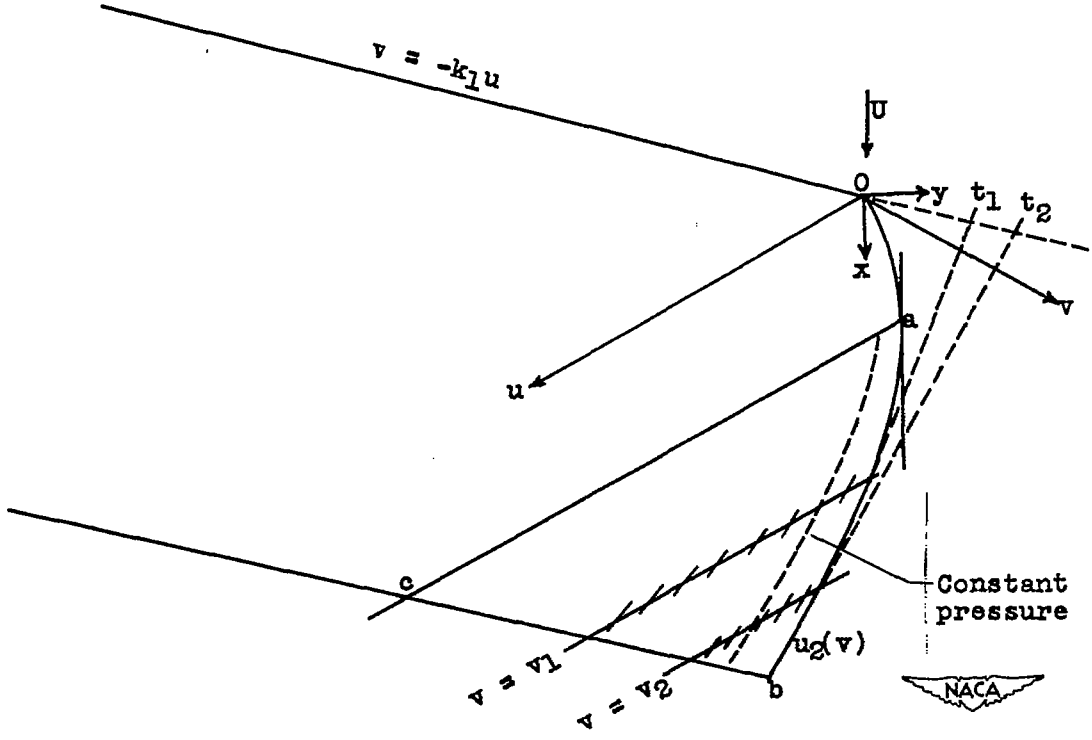

Figure 17. - Determination of constant-pressure lines for wing with straight supersonic leading edge in region influenced by subsonic trailing edge.